

Received February 21, 2022, accepted March 15, 2022, date of publication March 17, 2022, date of current version March 28, 2022.

Digital Object Identifier 10.1109/ACCESS.2022.3160467

# Tunable Filtenna With DGS Loaded Resonators for a Cognitive Radio System Based on an SDR Transceiver

**AHMED A. IBRAHIM**<sup>1</sup>, (Senior Member, IEEE),  
**HESHAM A. MOHAMED**<sup>2</sup>, (Senior Member, IEEE),  
**ALÁN RODRIGO DÍAZ RIZO**<sup>3</sup>, (Student Member, IEEE),  
**RAMON PARRA-MICHEL**<sup>4</sup>, (Member, IEEE),  
**AND HASSAN ABOUSHADY**<sup>3</sup>, (Senior Member, IEEE)

<sup>1</sup>Electronic Engineering Department, Minia University, El-Minia, Minya 61519, Egypt

<sup>2</sup>Electronics Research Institute (ERI), Cairo, Giza 12622, Egypt

<sup>3</sup>LJIP6 Laboratory, CNRS, Sorbonne University, 75231 Paris, France

<sup>4</sup>CINVESTAV, Guadalajara, Zapopan 45017, Mexico

Corresponding author: Ahmed A. Ibrahim (ahmedabdel\_monem@mu.edu.eg)

This work was supported in part by the French and Egyptian Governments through a Co-Financed Fellowship Grant by the French Embassy in Egypt (Institute Français d'Égypte), in part by the Scientific and Technology Development Fund (STDF) under Project 30642, and in part by the Franco-Mexican TOLTECA Project ANR-16-CE04-001301/CONACYT under Grant 273562.

**ABSTRACT** This paper introduces the design of a filtenna for cognitive radio systems. Four varactor diodes, which are inserted in the bandpass filter, are used to achieve the desired tunability. The proposed bandpass filter is integrated with a wideband monopole antenna. The bandpass filter is achieved by using two coupled defected ground structure (DGS) resonators and two coupled microstrip lines ended with two stubs. The monopole antenna is designed to operate in a frequency band from 1.3 GHz to 3 GHz. The four varactor diodes are used to tune the antenna resonance frequency from 2.7 GHz to 2 GHz when the capacitance increases from 1.55 pF to 2.67 pF. The performance of the proposed filtenna is validated by simulation and measurements from a fabricated prototype. Finally, the proposed filtenna is tested using the Software Defined Radio (SDR) platform bladeRF. This transceiver can transmit and receive in a wide frequency range of 0.3 GHz up to 3.8 GHz, which makes it suitable for testing the proposed reconfigurable filtenna.

**INDEX TERMS** Cognitive radio, reconfigurable antenna, wireless applications, lumped capacitors, RF transceivers, software defined radio.

## I. INTRODUCTION

Wireless devices able to modify their operating mode by self-aware of the environment are mandatorily required in recent years as they allow a Dynamic Spectrum Allocation (DSA) in wireless communication. This permits efficient use of the spectrum, which is the most scarce and valuable resource in modern wireless systems. The algorithms, devices and protocols devoted to managing with the DSA for interoperability of several wireless systems are grouped under the concept of Cognitive radio (CR) technology. According to FCC [1], CR means “real-time control of a radio channel or spectrum band and limiting rate, power or timing transmissions to

eliminate harmful interference with many other users of the spectrum” [2]. One of the most important hot topics for researchers is designing a reconfigurable broadband compact antenna device for CR applications [3]–[5]. The operation of a CR system is shown in Fig.1 [6], where it is shown that the radio must perform sensing of the RF environment, and after analysis and reasoning of the measurements, it follows an adaptation of its radio parameters to take benefits of the available resources to increase its performance. In CR, the configurability demand touches all layers of the design of wireless transceivers, but the area of designing a configurable antenna is particularly complex, as it involves the physical construction of antennas. Consider an intelligent radio system capable of detecting occupied and empty channels in the frequency spectrum [7]–[9], therefore, it is required

The associate editor coordinating the review of this manuscript and approving it for publication was Chinmoy Saha<sup>1</sup>.

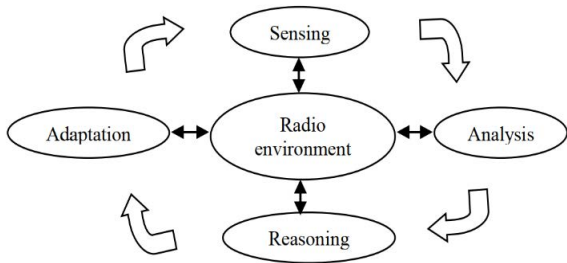


FIGURE 1. Block diagram of CR operation.

to include an antenna system capable of dealing with a broad RF Spectrum range. Two main approaches have been used, one type is the wideband antenna with a bandwidth covering the entire frequency band and the other type is the tunable narrow-band antenna with a wide tuning range. Therefore, for instance, to cover the RF range from 400MHz to 4 GHz, a compact and wireless reconfiguration antenna suitable for mobile devices is proposed in the spectral sensing of CR [10].

Recent research has been focusing on realizing some of the filtering functions in the antenna to reduce the constraints on the RF front-end and to reduce its complexity [11]. As reported in [12], [13], integrated filtering capabilities to achieve a wide impedance bandwidth by switching ON and OFF some parts of the antenna have been used. The antenna is capable of dynamically varying its properties using switches like PIN diodes, varactor diodes, or MEMS. These are frequently used components in the design of reconfigurable antennas [14], [15]. In these examples, the filtering is used to either insert a notch [16] to switch between several bands [17]–[19], or to switch within a wideband to narrowband subdivisions [20]. Also, the hardware implementations of the CR system are reported in [21]–[23]. Reference [21] discusses spectrum sensing algorithms based on friendly maximum-minimum eigenvalue for a CR network. In [22], VLSI algorithms based on blind spectrum sensing for maximum detection of eigenvalue are developed. Reference [23] investigates the development of hardware algorithms for cooperative spectrum sensing used for CR systems.

In this paper, a filtenna for CR systems is proposed. The fabricated filtenna has been measured and characterized using a Vector Network Analyzer (VNA). The filtenna has also been tested in a real CR environment using an SDR platform called bladeRF. The SDR operates in a frequency band from 0.3 GHz up to 3.8 GHz. The proposed filtenna is composed of a wideband monopole antenna attached to two coupled DGS bandpass filters. The antenna operates from 1.3 GHz to 3 GHz where tunability is achieved by loading four varactor diodes inside the DGS resonators to tune the antenna band from 2 GHz up to 3 GHz.

The innovation in this work is in two aspects. The first aspect is in combining the wideband antenna, introduced in Section II, with the varactor-based tunable bandpass filter,

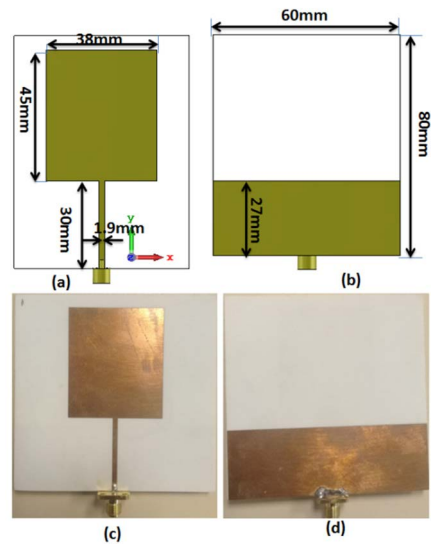


FIGURE 2. Wideband monopole antenna: (a) Top view (b) bottom view (c) Fabricated top view (d) Fabricated bottom view.

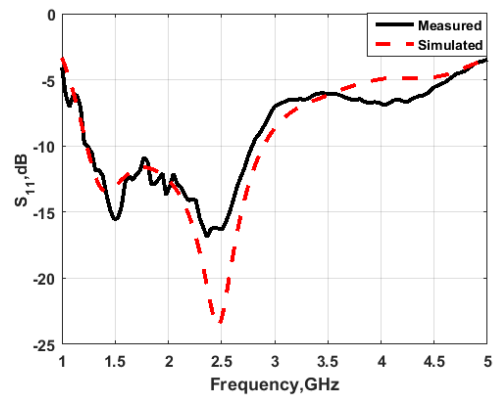


FIGURE 3.  $S_{11}$  simulated and measured results of the wideband monopole antenna.

presented in Section III, to create the proposed tunable filtenna, described in Section IV. The second aspect, described in Section V, is the use of this filtenna in a Cognitive Radio system based on a Software Defined Radio transceiver.

## II. WIDEBAND ANTENNA

In this section, a wideband antenna is taken as the initial design for the filtenna model as shown in Fig.2. The antenna is a monopole with a rectangular patch (front side). The wideband operation is accomplished by controlling the length of the partial ground plane (back side). The antenna is designed to work at a frequency band from 1.3 GHz up to 3 GHz which is suitable for the SDR platform bladeRF. The dimensions of the wideband antenna are optimized to cover the required frequency bands. The wideband antenna is printed on a Roger 4003 C substrate with dielectric constant, loss tangent and thickness of 3.38, 0.0027 and 0.813 mm, respectively. The feed-line width is chosen to produce the standard 50  $\Omega$  impedance. The wideband antenna is fabricated and

measured as shown in Fig.2 (c), (d). The antenna performance is measured using a VNA. The simulated and measured results for the wideband antenna are illustrated in Fig.3. It is clear that; first, the antenna has a bandwidth extended from 1.3 GHz up to 3 GHz with  $S_{11}$  lower than  $-10$  dB. Second, the simulated and measured results have the same trend which confirms the antenna design.

### III. BANDPASS FILTER

In this section, two coupled DGS resonators and a bandpass filter are introduced. The DGS is etched in the ground plane to produce current distributions which affect the capacitance and the inductance of the transmission line which enables it to operate as a combined bandstop / bandpass filter [24]–[26]. Fig. 4 depicts the proposed DGS bandpass filter. The bandpass filter consists of two L-shaped microstrip lines with a quarter-wavelength, as illustrated in Fig. 4(a), and two E-shaped back-to-back in the ground plane (E-DGS), as shown in Fig. 4(b). The two lumped RF capacitors are added to achieve the desired reconfigurability. First, the single DGS cell is designed to confirm the bandstop behavior of the DGS filter. Second, the proposed two coupled DGS, shown in Fig.4, are designed. The spaces between the two E-DGS and the two microstrip lines are optimized to fulfill the desired coupling coefficient and external quality factor. Compact frequency-reconfigurable filters are developed based on loaded resonators by lumped capacitors as described in [27], [28]. The proposed bandpass filter is designed simply with a standard, printed circuit board (PCB) technology. The copper traces are 0.035 mm thick and are etched on both sides of a Rogers 4003 C substrate, whose relative dielectric constant  $\epsilon_r = 3.38$ , relative permeability  $\mu_r = 1.0$ , loss tangent  $\tan \delta = 0.0027$  and a thickness of 0.813 mm. The two L-shaped microstrip coupling segments, whose characteristic impedance is  $50 \Omega$  with a width of 1.9 mm and  $S = 2.8$  mm. The optimized design parameters of the two E-DGS are illustrated in Fig.4(b). The resonance frequency of the filter can be easily shifted by adjusting the capacitor value. In Fig 5, the simulated  $S_{21}$ -parameters for the filter with  $C = 0.6$  pF are given in the dotted red curve, for  $C = 1$  pF are given in the black curve, and at  $C = 1.5$  pF are given in the dashed blue curve. It is seen that the center frequency of the filter can be controlled by changing the value of the lumped capacitor. The center frequency is shifted from 2.85 GHz, 2.45 GHz and 2.05 GHz when the capacitance values are changed to 0.6 pF, 1 pF and 1.5 pF respectively. A photo of the fabricated filter with two lumped capacitors of 1 pF is shown in Fig. 6.

We have used an RF Capacitor 388-6153-6-ND which has a typical value of 1 pF, and it is illustrated in Fig. 6. Simulation and measurement results are compared in Fig.7. The filter has a center frequency of 2.4 GHz, a 400 MHz bandwidth from 2.2 GHz to 2.6 GHz and a passband insertion loss and return loss of 0.45 dB and 20 dB respectively with a transmission zero at 2.95 GHz. This transmission zero is due to the two stubs of microstrip lines. Measurement results show that the filter has a good selectivity at passband/stopband edges.

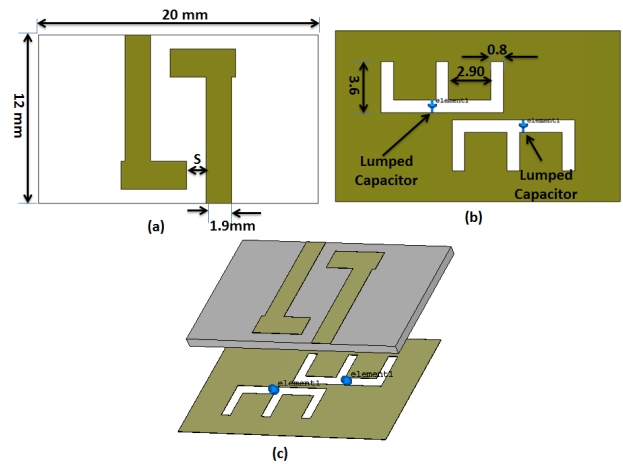


FIGURE 4. Bandpass filter with two lumped capacitors (a) Top view (b) bottom view. (c) 3D layout.

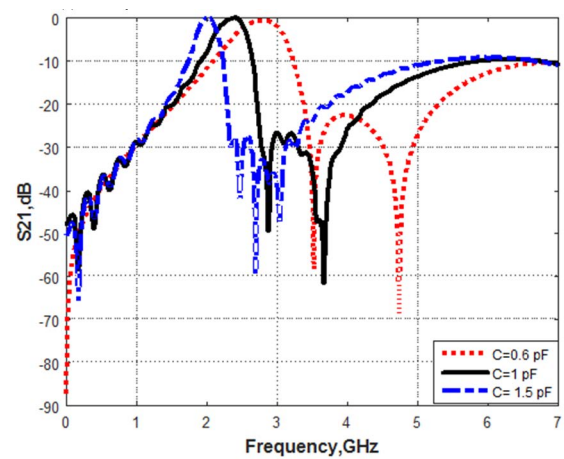


FIGURE 5. The Simulated  $S_{21}$  of the bandpass filter at different values of capacitance.

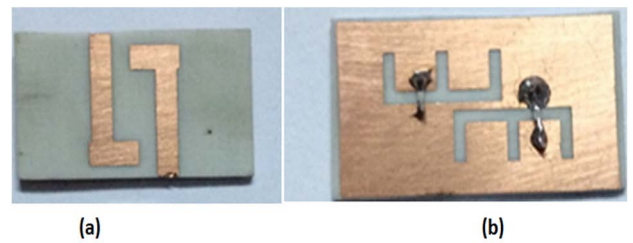


FIGURE 6. Fabricated photo of the bandpass filter (a) Top view (b) bottom view.

To achieve the desired reconfigurability to the proposed bandpass filter, varactor diodes are used instead of lumped capacitors. As shown in Fig. 8, the proposed bandpass filter discussed earlier in this Section should be modified to support varactor diodes in the DGS resonators. From Fig. 8, it can be observed that two copper strips with 3.2 mm length and 0.2 mm width are added inside the two DGS resonators and each resonator has two varactor diodes added in series. In Fig. 9, the simulated  $S_{21}$  parameters for the filter at

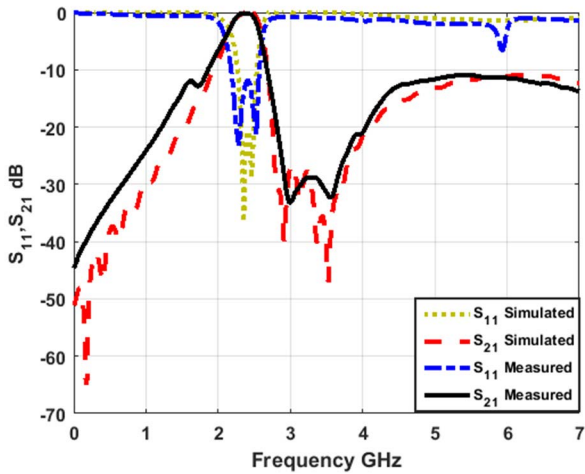


FIGURE 7. Simulated and measured results of bandpass filter at  $C=1$  pF.

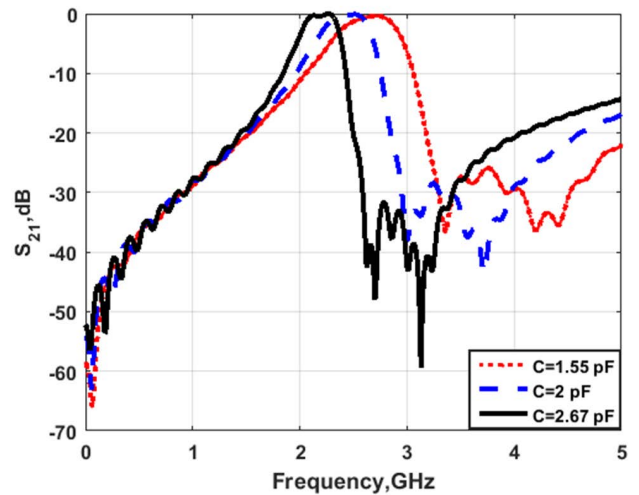


FIGURE 9. The Simulated  $S_{21}$  of the bandpass filter with four varactor diodes at different values of capacitance.

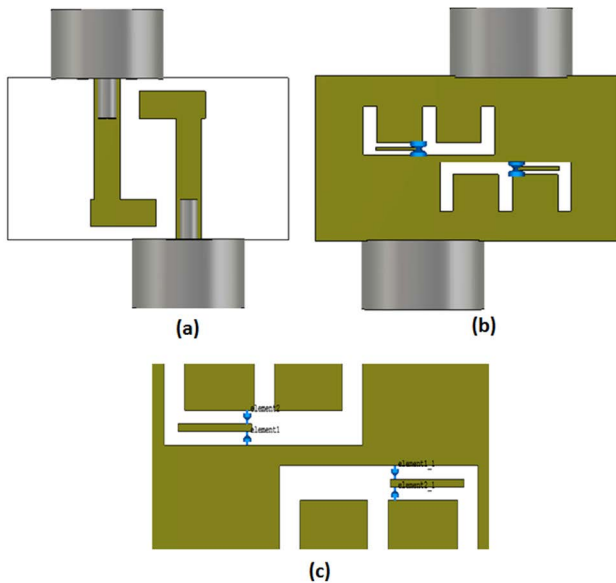


FIGURE 8. Bandpass filter with four varactor diodes: (a) Top view (b) bottom view (c) DGS slots with four varactor diodes.

$C = 1.55$  pF,  $C = 2$  pF and at  $C = 2.67$  pF are displayed. It is noticed that the center frequency is at 2.7 GHz, 2.45 GHz, and 2.2 GHz when the capacitance values are changed to 1.55 pF, 2 pF, and 2.67 pF respectively.

#### IV. PROPOSED FILTENNA

In this section, the wideband antenna is combined with the DGS bandpass filter with the four varactor diodes to produce the proposed filtenna. In Fig. 10 we show the fabricated filtenna. The filtenna  $S_{11}$  performance varies with the capacitance value of the lumped capacitors as illustrated in Fig. 11.

The antenna center frequency is changed from 2.65 GHz to 2.2 GHz when the capacitance is changed from 1.55 pF to 2.67 pF. The proposed filtenna is fabricated with four varactor diodes SMV1405 with capacitance ranging from

2.67 pF (with  $V_{VAR} = 0V$ ) to 1.55 pF (with  $V_{VAR} = 1.5$  V). The  $S_{11}$  simulation and measurement results of the proposed filtenna are illustrated in Fig. 12. Measurement results show that when  $V_{VAR} = 0V$ , the capacitance equals 2.67 pF and the region where  $S_{11}$  is lower than  $-10$  dB is extended from 2.07 GHz to 2.15 GHz, with a center frequency of 2.11 GHz (LTE2100). Measurements also show that when  $V_{VAR} = 0.5$  V, the capacitance is 2.12 pF and the region where  $S_{11}$  is lower than  $-10$  dB is extended from 2.27 GHz to 2.55 GHz with a center frequency of 2.41 GHz (ISM band and WiFi applications). Finally, when  $V_{VAR} = 1.5$  V, the capacitance is 1.55 pF and the region where  $S_{11}$  is lower than  $-10$  dB is extended from 2.57 GHz to 2.9 GHz with a center frequency of 2.735 GHz (LTE2600). From this figure, we can see that simulation and measurement results are very similar with a small shift due to fabrication process variations.

#### V. FILTENNA VALIDATION USING THE bladeRF SDR

BladeRF is an SDR platform developed by Nuand [29]. The LMS6002 transceiver enables the board to modify its analog front-end (AFE) through software, i.e. to set the RF center frequency (in the range from 0.3 - 3.8 GHz), to tune the gain (up to 56 dB for the transmitter and 61 dB for the receiver) and to select the desired bandwidth (from 1.5 MHz to 28MHz), among other configurations. It is also important to mention that transmitter signal path configuration is independent of receiver signal path. This allows the board to adapt itself to many wireless communication protocols.

Nevertheless, the architecture of the AFE contained in the LM6002 transceiver suffers from RF impairments, therefore, DC offset and IQ imbalance need to be digitally compensated to avoid the degradation of the overall system performance. A block diagram of the bladeRF board is shown in Fig. 13 [29]. The transmitter and the receiver chains of the bladeRF board have frequency-dependent gains; therefore, it is needed first to measure both the receiver

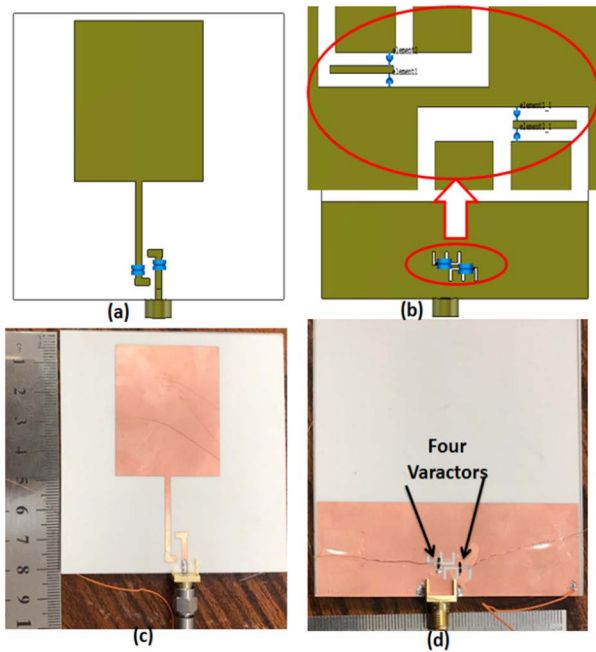


FIGURE 10. The proposed filtenna (a) 2 D layout top view (b) 2 D layout bottom view (c) Fabricated top view (d) Fabricated bottom view.

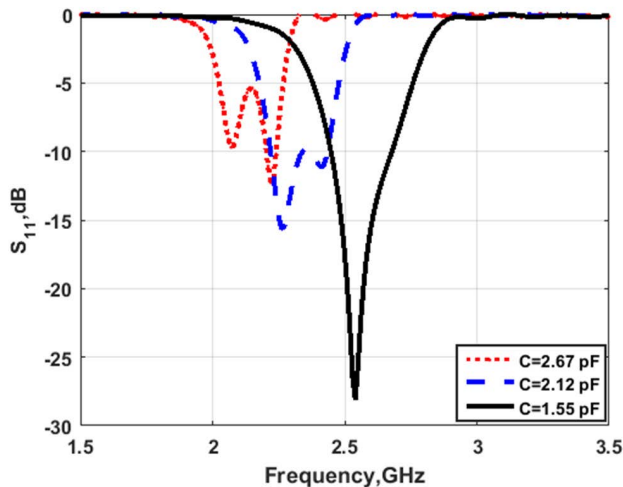


FIGURE 11.  $S_{11}$  simulation results of the filtenna with different values for the capacitance.

and the transmitter gains across the entire frequency of operation of the bladeRF. Using these measurements, the SDR board can be calibrated and then utilized for Spectrum Sensing (SS).

After finishing the calibration setup, the proposed filtenna is used at the receiver end of the SDR, as shown in Fig. 14. The bladeRF board using the proposed filtenna with  $V_{VAR} = 0V$ , is used to scan the spectrum from 2.06 GHz to 2.2 GHz in order to detect any busy channels in the LTE2100 band.

The result of this spectrum scanning is shown in Fig.15. From this figure, it can be seen that a few LTE2100 channels

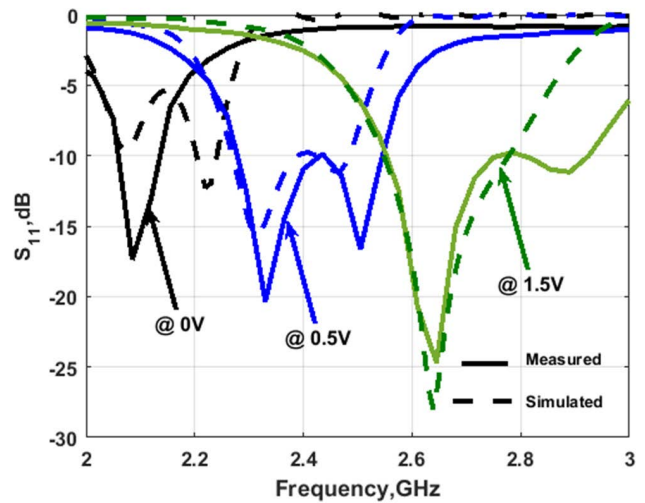


FIGURE 12. Simulation and measurement results of the filtenna with four varactors.

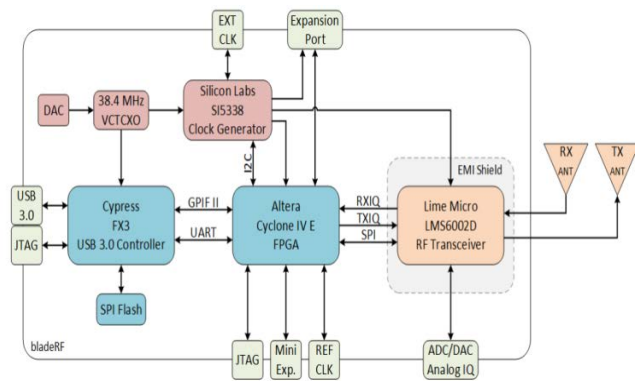


FIGURE 13. Block diagram of bladeRF SDR platform [29].

are busy at 2.06, 2.08 GHz and 2.15 GHz. We performed a second spectrum scanning, where the filtenna was tuned to the 2.4 GHz (ISM-band). The result of this spectrum scanning is shown in 2-D in Fig. 16 and 3-D, as a function of time, in Fig. 17. From these figures, it can be seen that a few WiFi channels are busy at 2.43 GHz, 2.44 GHz and 2.45 GHz. In Fig.17, the filtering effect of the filtenna can clearly be seen on the out-of-band frequencies.

Finally, we employed the proposed filtenna (at  $V_{VAR} = 1.5 V$ ) and the bladeRF board to scan the spectrum from 2.65 GHz to 2.75 GHz in order to detect a transmitted signal using a monopole antenna operated around this frequency band. The results of this spectrum scanning are shown Fig. 18.

It can be seen that a few channels are busy at 2.68 GHz, 2.69 GHz, 2.7 GHz and 2.71 GHz.

In order to simulate a Cognitive Radio scenario, we generated six QPSK-modulated signals, up-converted them to six different center frequencies and transmitted them using the bladeRF transmitter connected to a standard monopole antenna. At the receiver side of the bladeRF board, we used the proposed filtenna. For the experiment, we ensured that

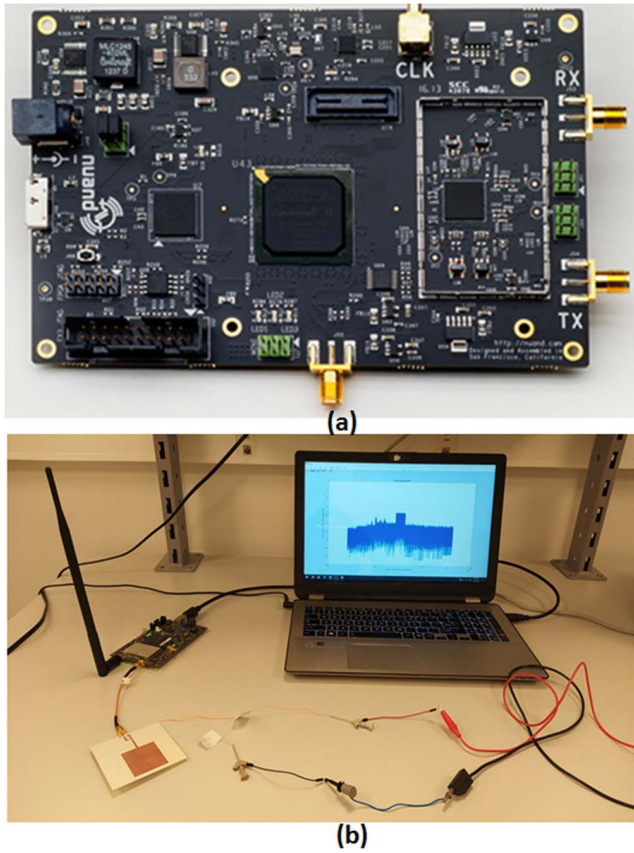


FIGURE 14. (a) The bladeRF SDR Board (b) The proposed filtenna connected to the receiver port of the bladeRF.

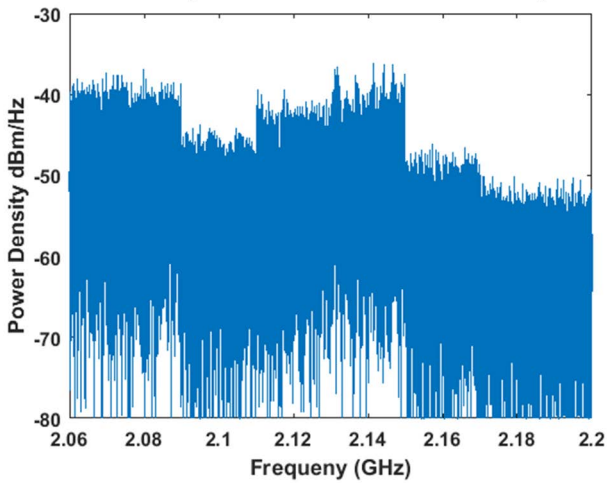


FIGURE 15. Spectrum Sensing from 2.06 GHz to 2.2 GHz at  $V_{VAR} = 0$  V using the proposed filtenna at the receiver of the bladeRF SDR board.

the receiving filtenna was placed at the far field propagation scenario (around 120 cm), and this experiment was operated in an isolated room to reduce interference with other 2.46 GHz applications. The Power Spectral Density (PSD) of the received signal is plotted in Fig. 19. From this figure, it can

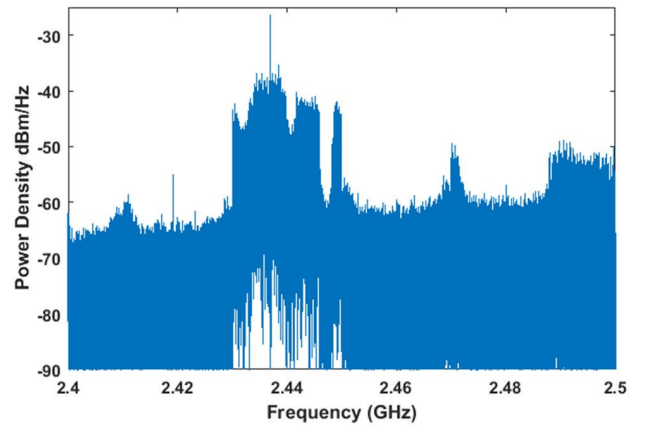


FIGURE 16. Spectrum Sensing from 2.4GHz to 2.5 GHz at  $V_{VAR} = 0.5$  V using the proposed filtenna at the receiver of the bladeRF SDR board.

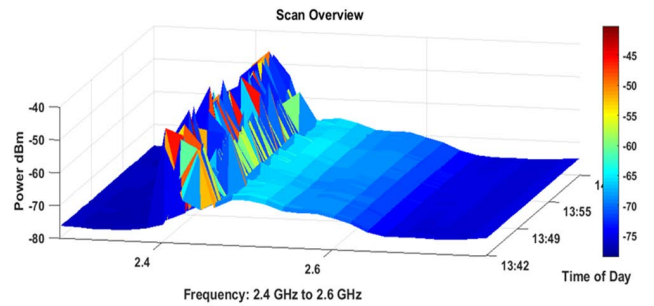


FIGURE 17. Spectrum Sensing from 2.4 GHz to 2.6 GHz at  $V_{VAR} = 0.5$  V in function of time. Measurements performed using the proposed filtenna at the receiver end of the bladeRF SDR board.

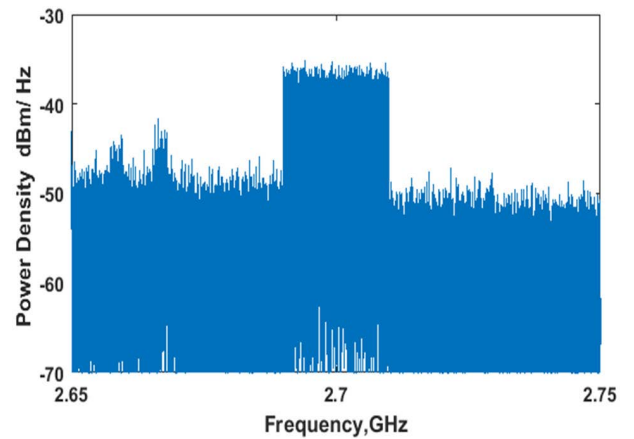
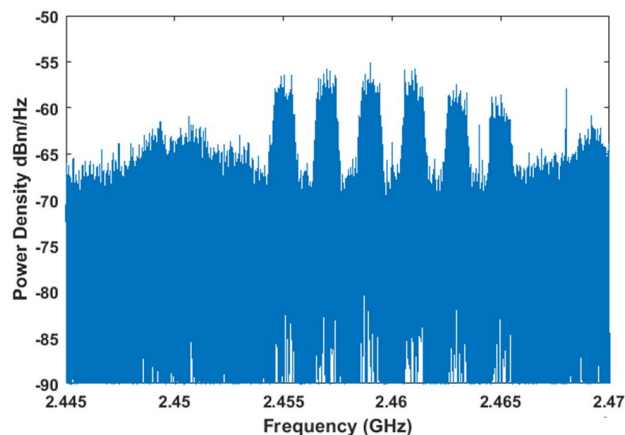
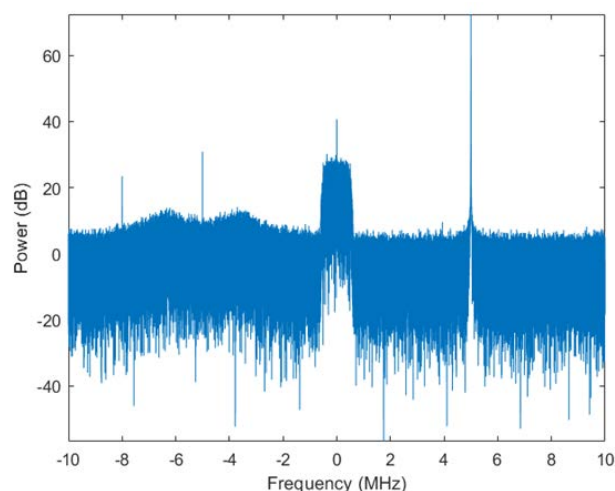


FIGURE 18. Spectrum Sensing from 2.65GHz to 2.75 GHz using the proposed filtenna at the receiver end of the bladeRF SDR board.

be concluded that the proposed filtenna can be used for spectrum sensing applications, e.g., to detect spectral occupancy. The SDR can then decide the best channel to use to establish communication. The filtenna center frequency can be tuned by changing the capacitance of the four varactor diodes by



**FIGURE 19.** Spectral power density of the 6 pulses transmitted using monopole antenna and received by using the proposed filtenna at  $V_{VAR} = 0.5$  V.



**FIGURE 20.** Received baseband spectrum of the single-carrier QPSK signal using the proposed filtenna at 2.1 GHz  $V_{VAR} = 0.0$  V.

changing the applied voltage. The proposed filtenna is also suitable for different SDR architectures, like highly digitized receivers based on RF ADCs [30].

Now that the Spectrum Sensing operation is validated, it is necessary to evaluate the performance of the filtenna in establishing wireless communication. To demonstrate this function, we generated a single-carrier QPSK signal transmitted at 2.1 GHz using a monopole antenna at the transmitting end of the bladeRF board. The transmitted signal is then received using the proposed filtenna at 2.1 GHz ( $V_{VAR} = 0V$ ). Fig. 20 shows the received down-converted spectrum using the proposed filtenna and Fig. 21 shows the received QPSK constellation. After QPSK demodulation, the measured Bit Error Rate (BER) of the receiver signal is zero, which shows that the proposed filtenna can be used to perform wireless communications.

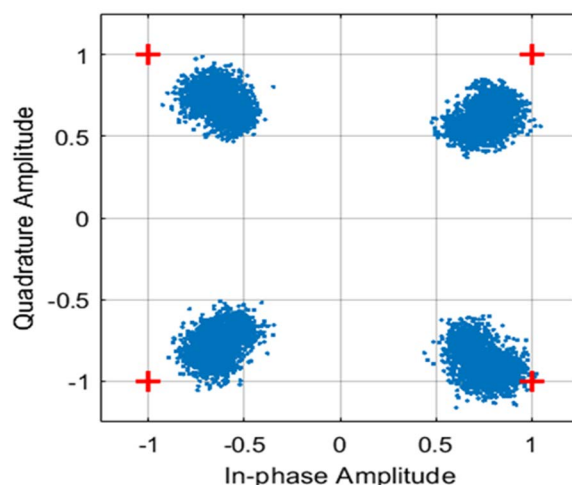


**FIGURE 21.** Received constellation of the single-carrier QPSK signal using the proposed filtenna at 2.1 GHz  $V_{VAR} = 0.0$  V.

## VI. CONCLUSION

A filtenna for Cognitive Radio applications has been fabricated, measured and tested using the bladeRF SDR platform. First a wideband antenna has been designed to operate at frequency band 1.3 GHz up to 3 GHz. Second, two Defected Ground Structure resonators loaded with lumped capacitors bandpass filter have been designed, fabricated and measured at different center frequencies. Third, the wideband antenna has been combined with the bandpass filter and four varactor diodes to obtain the desired tunable filtenna. The proposed filtenna has been tested and validated using the bladeRF SDR platform. The proposed filtenna has been used in the receiver to sense the spectrum around 2.1, 2.4, 2.7 GHz by changing the varactor voltage from 0, 0.5, 1.5 V respectively. The proposed filtenna has also been used to receive a QPSK-modulated signal transmitted from another antenna.

## REFERENCES

- [1] *Report of the Spectrum Efficiency Working Group*, Federal Communications Commission, FCC Spectrum Policy Task Force, Washington, DC, USA, 2002.
- [2] Y. Tawk, J. Costantine, and C. G. Christodoulou, "Cognitive-radio and antenna functionalities: A tutorial," *IEEE Antennas Propag. Mag.*, vol. 56, no. 1, pp. 231–243, Feb. 2014.
- [3] N. Kumar, P. A. Raju, and S. K. Behera, "Frequency reconfigurable microstrip antenna for cognitive radio applications," in *Proc. Int. Conf. Commun. Signal Process. (ICCSPP)*, Apr. 2015, pp. 370–373.
- [4] B. P. Chacko, G. Augustin, and T. A. Denidni, "Electronically reconfigurable uniplanar antenna with polarization diversity for cognitive radio applications," *IEEE Antennas Wireless Propag. Lett.*, vol. 14, pp. 213–216, 2015.
- [5] A. Shanmukha, S. Pavan, and S. P. Reddy, "Frequency reconfigurable microstrip patch antenna for cognitive radio applications," *Int. J. Adv. Res. Electr., Electron. Instrum. Eng.*, vol. 6, no. 3, pp. 1052–1057, 2017.
- [6] M. Abirami and A. Vimala, "A review of various antenna design methods for cognitive radio application," in *Proc. 4th Int. Conf. Electron. Commun. Syst. (ICECS)*, Feb. 2017, pp. 117–120.
- [7] O. El Maleky, F. Ben Abdelouahab, M. Essaadi, and L. Ajana, "Reconfigurable T-shaped antenna for S-band applications," in *Proc. 5th Int. Conf. Multimedia Comput. Syst. (ICMCS)*, Sep. 2016, pp. 451–455.
- [8] S. Arivazhagan, R. AhilPriyadarshini, and V. Shanthi Devi, "Design of a reconfigurable antenna for cognitive radio," in *Proc. IEEE Int. Conf. Electr., Comput. Commun. Technol. (ICECCT)*, Mar. 2015, pp. 1–5.

- [9] M. Shirazi, T. Li, and X. Gong, "A new design of reconfigurable slot-ring antenna using PIN diodes," in *Proc. IEEE Int. Symp. Antennas Propag. USNC/URSI Nat. Radio Sci. Meeting*, Jul. 2015, pp. 2271–2272.
- [10] S. Ershadi, A. H. Abdelrahman, M. Liang, X. Yu, H. Xin, and S. Ershadi, "A novel reconfigurable broadband antenna for cognitive radio systems," in *Proc. IEEE Int. Symp. Antennas Propag. (APSURSI)*, Jun. 2016, pp. 1799–1800.
- [11] B. Zhang and Q. Xue, "Filtering antenna with high selectivity using multiple coupling paths from source/load to resonators," *IEEE Trans. Antennas Propag.*, vol. 66, no. 8, pp. 4320–4325, Aug. 2018.
- [12] M. E. Yassin, H. A. Mohamed, E. A. F. Abdallah, and H. S. El-Hennawy, "Circularly polarized wideband-to-narrowband switchable antenna," *IEEE Access*, vol. 7, pp. 36010–36018, 2019.
- [13] A. Valizade, C. Ghobadi, J. Nourinia, and M. Ojaroudi, "A novel design of reconfigurable slot antenna with switchable band notch and multiresonance functions for UWB applications," *IEEE Antennas Wireless Propag. Lett.*, vol. 11, pp. 1166–1169, 2012.
- [14] Y. Tawk, J. Costantine, and C. G. Christodoulou, "Cognitive-radio and antenna functionalities: A tutorial," *IEEE Antennas Propag. Mag.*, vol. 56, no. 1, pp. 231–243, Feb. 2014.
- [15] C. Saha, J. Y. Siddiqui, A. P. Freundorfer, L. A. Shaik, and Y. M. M. Antar, "Active reconfigurable ultra-wideband antenna with complementary frequency notched and narrowband response," *IEEE Access*, vol. 8, pp. 100802–100809, 2020.
- [16] W. A. Ali, H. A. Mohamed, A. A. Ibrahim, and M. Z. Hamdalla, "Gain improvement of tunable band-notched UWB antenna using metamaterial lens for high speed wireless communications," *Microsyst. Technol.*, vol. 25, pp. 4111–4117, Nov. 2019.
- [17] G. Augustin, B. P. Chacko, and T. A. Denidni, "Electronically reconfigurable uni-planar antenna for cognitive radio applications," *IET Microw., Antennas Propag.*, vol. 8, no. 5, pp. 367–376, Apr. 2014.
- [18] M.-C. Tang, Z. Wen, H. Wang, M. Li, and R. W. Ziolkowski, "Compact, frequency-reconfigurable filtenna with sharply defined wideband and continuously tunable narrowband states," *IEEE Trans. Antennas Propag.*, vol. 65, no. 10, pp. 5026–5034, Oct. 2017.
- [19] H. Nachouane, A. Najid, F. Riouch, and A. Tribak, "Electronically reconfigurable filtenna for cognitive radios," *Microw. Opt. Technol. Lett.*, vol. 59, no. 2, pp. 399–404, Feb. 2017.
- [20] N. O. Parchin, H. J. Basherlou, Y. Al-Yasir, R. Abd-Alhameed, A. Abdulkhaleq, and J. Noras, "Recent developments of reconfigurable antennas for current and future wireless communication systems," *Electronics*, vol. 8, no. 2, p. 128, Jan. 2019.
- [21] R. B. Chaurasiya and R. Shrestha, "Hardware-efficient and fast sensing-time maximum-minimum-eigenvalue-based spectrum sensor for cognitive radio network," *IEEE Trans. Circuits Syst. I, Reg. Papers*, vol. 66, no. 11, pp. 4448–4461, Nov. 2019.
- [22] R. B. Chaurasiya and R. Shrestha, "Fast sensing-time and hardware-efficient eigenvalue-based blind spectrum sensors for cognitive radio network," *IEEE Trans. Circuits Syst. I, Reg. Papers*, vol. 67, no. 4, pp. 1296–1308, Apr. 2020.
- [23] R. B. Chaurasiya and R. Shrestha, "A new hardware-efficient spectrum-sensor VLSI architecture for data-fusion-based cooperative cognitive-radio network," *IEEE Trans. Very Large Scale Integr. (VLSI) Syst.*, vol. 29, no. 4, pp. 760–773, Apr. 2021.
- [24] A. Boutejdar, A. A. Ibrahim, and E. P. Burte, "DGS resonators form compact filters," *Microw. RF*, vol. 54, no. 3, pp. 52–60, 2015.
- [25] A. Boutejdar, A. A. Ibrahim, and E. P. Burte, "Design of a novel ultrawide stopband lowpass filter using a DMS-DGS technique for radar applications," *Int. J. Microw. Sci. Technol.*, vol. 2015, pp. 1–7, Oct. 2015.
- [26] H. A. E. Mohamed, H. B. El-Shaarawy, E. A.-F. Abdallah, and H. M. El-Hennawy, "Design of reconfigurable miniaturized UWB-BPF with tuned notched band," *Prog. Electromagn. Res. B*, vol. 51, pp. 347–365, 2013.
- [27] A. A. Ibrahim, H. A. Mohamed, and W. A. E. Ali, "Tunable dual/triple band-pass filter based on stub-loaded resonators for wireless applications," *J. Instrum.*, vol. 12, pp. 1–12, Apr. 2017.
- [28] A. Boutejdar and A. A. W. A. E. Ibrahim Ali, "Design of compact size and tunable bandpass filter for WLAN applications," *Electron. Lett.*, vol. 52, no. 24, 1996–1997, 2016.
- [29] Nuand. (2018). *BladeRF—The Usb 3.0 Superspeed Software Defined Radio*. [Online]. Available: <http://nuand.com/>
- [30] A. Sayed, T. Badran, M.-M. Louerat, and H. Aboushady, "A 1.5-to-3.0GHz tunable RF sigma-delta ADC with a fixed set of coefficients and a programmable loop delay," *IEEE Trans. Circuits Syst. II, Exp. Briefs*, vol. 67, no. 9, pp. 1559–1563, Sep. 2020.



**AHMED A. IBRAHIM** (Senior Member, IEEE) was born in 1986. He received the B.Sc., M.Sc., and Ph.D. degrees in electrical engineering from the Electronic and Communication Engineering Department, Minia University, Elminia, Egypt, in 2007, 2011, and 2014, respectively. He is currently an Associated Professor with the Electrical Engineering Department, Faculty of Engineering, Minia University. He has been a Visiting Professor at University Pierre and Marie Curie; Sorbonne University, Paris VI, France, for seven months; and Otto-von-Guericke-Universität Magdeburg, Germany, for six months. He has published more than 95 peer-reviewed journals and conference papers. His research interests include miniaturized multiband antennas/wideband, microwave/millimeter components, DRA metamaterial antenna, graphene antenna, microwave filters, MIMO antennas, and energy harvesting systems. He is a Senior Member of URSI and a member of the National Committee of Radio Science, Egypt. He is currently a Reviewer of IEEE ANTENNAS AND WIRELESS PROPAGATION LETTERS, IEEE MICROWAVE WIRELESS COMPONENTS, IEEE ACCESS, IET Microwave, Antenna and Propagation, IET Electronics Letters, MOTL, Analog Integrated Circuits and Signal Processing, and many others journal and conferences.



**HESHAM A. MOHAMED** (Senior Member, IEEE) received the B.Sc. degree in electronics and communication engineering from the University of Menofia, in 2003, and the M.Sc. and Ph.D. degrees from Ain Shams University, in 2009 and 2014, respectively. He is currently a Researcher with the Electronics Research Institute (ERI), Giza, Egypt. He has teaching experience of more than 12 years'. He was a Lecturer with the Electronic and Communication Engineering Department, Faculty of Engineering, Misr University for Science and Technology. He has authored or coauthored close to 25 journal articles, about 19 refereed conference papers, and attend and chaired several national and international conferences. He has supervised and co-supervised four Ph.D. and three M.Sc. theses at Cairo University, Ain Shams University, and Helwan University. His outstanding publications of work is ranked in international journals and conferences. His research interests include microwave circuit designs, planar antenna systems, recently on EBG structures, UWB components and antenna and RFID systems, radar Absorbing materials, energy harvesting and wireless power transfer, smart antennas, microstrip antennas, microwave filters, metamaterials, and MIMO antennas and its applications in wireless communications. He is a Reviewer of the international journals, such as IEEE MICROWAVE AND WIRELESS COMPONENTS LETTERS, IEEE ACCESS, *Progress in Electromagnetics Research Letters (PIER, PIER B, C, M, PIER Letters)*, *Microwave and Optical Technology Letters*, and *International Journal of Circuit Theory and Applications*.



**ALÁN RODRIGO DÍAZ RIZO** (Student Member, IEEE) received the B.S. degree in electronics and communication engineering from Guadalajara University, Guadalajara, Mexico, in 2015, and the M.S. degree in electrical engineering from the Center for Research and Advanced Studies of the National Polytechnic Institute (Cinvestav), Guadalajara, in 2018. He is currently pursuing the Ph.D. degree with Sorbonne University, Paris, France. His research interests include hardware security, cognitive radio, and radio signal processing.





**RAMON PARRA-MICHEL** (Member, IEEE) was born in Guadalajara, Mexico, in 1973. He received the B.Sc. degree in electronics and communications from the University of Guadalajara, Jalisco, Mexico, in 1996, the M.Sc. degree in electrical engineering, specializing in communications, from CINVESTAV-IPN, Guadalajara, in 1998, and the Ph.D. degree in electrical engineering specialized in digital signal processing for communications from CINVESTAVIPN, Mexico City, Mexico, in 2003. He has collaborated with several companies and institutions either in academic or technology projects, such as Siemens, Lucent, Mabe, Mixbaal, Hewlett-Packard, and Intel. He is currently a Full Member of Research Staff with CINVESTAV-IPN, Guadalajara Unit. His research interests include modeling, simulation, estimation and equalization of communication channels, and digital implementation of DSP algorithms for communication systems.



**HASSAN ABOUSHADY** (Senior Member, IEEE) received the B.Sc. degree in electrical engineering from Cairo University, Egypt, in 1993, and the M.Sc. and Ph.D. degrees in electrical engineering and computer science and the H.D.R. degree from Sorbonne University, Paris, France, in 1996, 2002, and 2010, respectively.

He is currently an Associate Professor with Sorbonne University. He worked on the design of digital-to-analog and analog-to-digital converters at NXP, Eindhoven, The Netherlands, and STMicroelectronics, Crolles, France. He was a Visiting Professor for several months at French University (UFE), Egypt, in 2007; the Federal University of Rio Grande do Norte (UFRN), Brazil, in 2011; and the Technologico de Monterrey (ITESM), Guadalajara, Mexico, in 2012; and Ecole Polytechnique (LPICM), Palaiseau, France, in 2013. His research interests include sigma-delta modulation, analog/RF circuit design, analog-to-digital and digital-to-analog conversion, and security in analog and mixed-signal circuits. He is the author and coauthor of more than 80 publications in these areas. He was a recipient of the 2004 Best Paper Award in the IEEE Design Automation and Test in Europe Conference and the recipient and the co-recipient of the second and the third best student paper awards of the IEEE Midwest Symposium on Circuits and Systems, in 2000 and 2003, respectively. He is an IEEE-CAS Distinguished Lecturer and a member of the IEEE Circuits and Systems for Communications Committee (CASCOM). He also served as an Associate Editor for the IEEE TRANSACTIONS ON CIRCUITS AND SYSTEMS—II: EXPRESS BRIEFS.

• • •